Comparative Biochemistry and Physiology, Part C 162 (2014) 77–84

Contents lists available at ScienceDirect

Comparative Biochemistry and Physiology, Part C

journal homepage: www.elsevier.com/locate/cbpc

Transient modulation of acetylcholinesterase activity caused by exposure to dextran-coated iron oxide nanoparticles in brain of adult zebrafish

Giovanna Medeiros Tavares de Oliveira [a], Luiza Wilges Kist [a,b], Talita Carneiro Brandão Pereira [a], Josiane Woutheres Bortolotto [c], Francisco Lima Paquete [d], Elisa Magno Nunes de Oliveira [d], Carlos Eduardo Leite [e], Carla Denise Bonan [b,c], Nara Regina de Souza Basso [d], Ricardo Meurer Papaleo [d], Maurício Reis Bogo [a,b,e,*]

[a] Laboratório de Biologia Genômica e Molecular, Faculdade de Biociências, Pontifícia Universidade Católica do Rio Grande do Sul, Avenida Ipiranga, 6681, 90619-900 Porto Alegre, RS, Brazil
[b] Instituto Nacional de Ciência e Tecnologia Translacional em Medicina (INCT-TM), Porto Alegre, RS, Brazil
[c] Laboratório de Neuroquímica e Psicofarmacologia, Faculdade de Biociências, Pontifícia Universidade Católica do Rio Grande do Sul, Avenida Ipiranga, 6681, 90619-900 Porto Alegre, RS, Brazil
[d] Laboratório de Síntese de Materiais Nanoestruturados, Faculdade de Física, Pontifícia Universidade Católica do Rio Grande do Sul, Avenida Ipiranga, 6681, 90619-900 Porto Alegre, RS, Brazil
[e] Instituto de Toxicologia e Farmacologia, Pontifícia Universidade Católica do Rio Grande do Sul, Avenida Ipiranga, 6681, 90619-900 Porto Alegre, RS, Brazil

ARTICLE INFO

Article history:
Received 21 August 2013
Received in revised form 14 March 2014
Accepted 27 March 2014
Available online 2 April 2014

Keywords:
SPIONs
CLIO-NH_2
AChE
Neurotoxicity
Apoptosis
Zebrafish

ABSTRACT

Superparamagnetic iron oxide nanoparticles (SPIONs) are of great interest in nanomedicine due to their capability to act simultaneously as a contrast agent and as a targeted drug delivery system. At present, one of the biggest concerns about the use of SPIONs remains around its toxicity and, for this reason, it is important to establish the safe upper limit for each use. In the present study, SPION coated with cross-linked aminated dextran (CLIO-NH_2) were synthesized and their toxicity to zebrafish brain was investigated. We have evaluated the effect of different CLIO-NH_2 doses (20, 50, 100, 140 and 200 mg/kg) as a function of time after exposure (one, 16, 24 and 48 h) on AChE activity and *ache* expression in zebrafish brain. The animals exposed to 200 mg/kg and tested 24 h after administration of the nanoparticles have shown decreased AChE activity, reduction in the exploratory performance, significantly higher level of ferric iron in the brains and induction of *casp8*, *casp 9* and *jun* genes. Taken together, these findings suggest acute brain toxicity by the inhibition of acetylcholinesterase and induction of apoptosis.

1. Introduction

Magnetic nanoparticles (MNPs) have attracted great interest in recent years due to their unique physical and chemical properties and their potential applications in various biomedical fields (Lu et al., 2007). They consist of small domains (usually smaller than 100 nm), containing magnetic atoms such as iron, cobalt or nickel that can be easily manipulated using an external magnetic field (Wang et al., 2001). Among magnetic nanoparticles, the superparamagnetic iron oxide nanoparticles (SPIONs) are of particular interest on account of the strong magnetic response when the particles are exposed to an external magnetic field and, the lack of residual magnetization when the field is removed. In addition, these particles present biocompatibility, injectability, and may have a high rate of accumulation in the target tissue if adequate ligands are attached to their surfaces (Ito et al., 2005). SPIONs have found a great number of biomedical applications; for instance, as contrast agents in magnetic resonance imaging, in magnetic separation of cells and proteins, in drug and gene delivery, in anticancer treatments by hyperthermia and tissue engineering (Singh et al., 2010).

Surface characteristics such as size and shape affect the toxicological profile of the nanoparticles (NPs) and their overall *in vivo* behavior (Chouly et al., 1996). For this reason, it is important to establish the safe upper limit for each use. Diverse aspects of the *in vitro* toxicity including, cytotoxicity, genotoxicity and oxidative stress generation and some general aspects of the *in vivo* toxicity of SPIONs, were investigated (for review, see Mahmoudi et al., 2012). For instance, rats that had been intravenously injected with γ-Fe_2O_3 NPs (0.8 mg/kg) presented toxicity in liver, kidneys and lungs (Hanini et al., 2011). Acute oral exposure to Fe_2O_3-30 NPs caused more than 50% inhibition of total $Na^{(+)}$–$K^{(+)}$, $Mg^{(2+)}$, and $Ca^{(2+)}$-ATPase activities in brains of female rats and activation of the hepatotoxicity marker enzymes, aspartate aminotransferase and alanine aminotransferase in serum and liver (Kumari et al., 2013). In accordance, due to Fe_2O_3-30 NPs 28 days repeated oral dose,

* Corresponding author at: Faculdade de Biociências, Pontifícia Universidade Católica do Rio Grande do Sul, Avenida Ipiranga, 6681-12C, Sala 134, 90619-900, Porto Alegre, RS, Brazil. Tel.: +55 51 3353 4726; fax: +55 51 3320 3568.
E-mail address: mbogo@pucrs.br (M.R. Bogo).

http://dx.doi.org/10.1016/j.cbpc.2014.03.010
1532-0456/

significant inhibition was observed in total $Na^{(+)}$–$K^{(+)}$, $Mg^{(2+)}$, and $Ca^{(2+)}$-ATPase activities in the brain of exposed rats (Kumari et al., 2012). Developmental toxicity causing mortality, hatching delay, and malformation were found in zebrafish (*Danio rerio*) embryos exposed to higher doses than 10 mg/L of iron oxide nanoparticles (Zhu et al., 2012).

In cholinergic neurotransmission, acetylcholine (ACh) promotes the activation of muscarinic and nicotinic cholinergic receptors. The maintenance of levels of ACh in the extracellular space is catalyzed by acetylcholinesterase (AChE) and butyrylcholinesterase (BuChE), by the hydrolysis of ACh into its component parts choline and acetate (Soreq and Seidman, 2001). It has been demonstrated that BuChE is not encoded in the zebrafish genome, but AChE is encoded by a single gene that has been functionally detected in zebrafish brain (Bertrand et al., 2001). The inhibition of AChE activity for assessment of the exposure of organisms to organophosphate and carbamate pesticides is well-known (for review see Van Dyk and Pletschke, 2011). However, other toxic compounds than organophosphate and carbamate pesticides both promoted AChE inhibition and AChE activation in fish. For instance, the inhibition of zebrafish brain AChE activity by neurotoxic compounds such as methanol (Rico et al., 2006), lithium (Oliveira et al., 2011), the heavy metals mercury and lead (Richetti et al., 2011), and the organochlorine pesticide Endosulfan (Pereira et al., 2012) has been demonstrated. Notwithstanding, AChE activation has also been demonstrated as a consequence of exposure to toxic substances such as ethanol (Rico et al., 2007), aluminum (Senger et al., 2011) and Microcystin-LR (Kist et al., 2012).

Thus, considering that (1) SPIONs have been developed for a number of applications; (2) it is crucial to establish the safe upper limit for each SPION's use; (3) the *in vivo* neurotoxic effects of SPIONs are not completely understood; (4) AChE activity is successfully used as a biomarker of brain injury, the aim of the present study was to evaluate the effects caused by exposure to dextran-coated SPIONs in the brain using adult zebrafish as the organism model.

2. Materials and methods

2.1. Animals

Adult wild-type zebrafish (*D. rerio*, Cyprinidae) of both sexes (6–9 months-old) were obtained from a specialized supplier (Redfish Agroloja, RS, Brazil). Animals were kept at a density of up to five animals per liter in 50 L housing tanks with tap water that was previously treated with Tetra's AquaSafe® (to neutralize chlorine, chloramines, and heavy metals present in the water that could be harmful to fish) and continuously aerated (7.20 mg O_2/L) at 26 ± 2 °C, under a 14/10 h light/dark controlled photoperiod. Animals were acclimated for at least two weeks before the experiments and were fed three times a day with TetraMin Tropical Flake fish food®. The fish were maintained healthy and free of any signs of disease and were used according to the "Guide for the Care and Use of Laboratory Animals" published by the US National Institutes of Health. All procedures in the present study were approved by the Animal Ethics Committee of the Pontifical Catholic University of Rio Grande do Sul (PUCRS), protocol number 12/00288.

2.2. Chemicals

Trizma Base, ethylene-dioxy (EDTA), ethylene glycol bis (beta amino ethylether)-N,N,N′,N′-tetraacetic acid (EGTA), sodium citrate, Coomassie Blue G, bovine serum albumin, acetylthiocholine, and 5,5′-dithiobis-2-nitrobenzoic acid (DTNB) were purchased from Sigma Aldrich Chemical Co (St. Louis, MO, USA). TRIzol® reagent, ImPROm-II Reverse Transcriptase® (Promega, Madison, Wisconsin, USA), Platinum® Taq DNA Polymerase and GelRed® were purchased from Invitrogen (Carlsbad, CA, USA).

2.3. Dextran coated SPION synthesis and characterization

Iron oxide (Fe_3O_4) nanoparticles coated with cross linked aminated dextran (CLIO-NH_2) were synthesized by the co-precipitation method in an alkaline environment, based on the procedure described previously (Wunderbaldinger et al., 2002). The synthesis was made by dissolution of dextran (T10, pharmacosmos) in an aqueous medium and mixed with salts of $FeCl_3.6H_2O$ and $FeCl_2.4H_2O$ (Merck) with a molar ratio of 2:1, in a cold environment and N_2 flux. NH_4OH (25%, Merck) was added slowly in the solution and stirred at 75–85 °C for 90 min. To eliminate the excess dextran, the mixture was centrifuged in Amicon® filters with a molecular mass cutoff of 50 kDa. Cold 5 M NaOH (Merck) was added slowly and stirred for 15 min and then epichlorohydrin (Fluka) was added for the crosslinking of the dextran chains. For amination of the dextran coating, NH_4OH (25%, Merck) was added in the NP solution and stirred for additional 24 h. After that, the remaining NH_4OH was eliminated by dialysis, using cellulose membranes (Spectra/Por®) submerged in distilled water under continuous magnetic stirring. Water was exchanged several times in this process. The resulting CLIO-NH_2 nanoparticles were dispersed in sodium citrate buffer (10 mM $Na_3C_6H_5O_7$/150 mM NaCl) at pH 8 and stored at 4 °C.

For characterization, all samples were initially sonicated (40 kHz) and stirred in a vortex and then the desired aliquots collected. Iron concentration was determined by UV–vis spectroscopy (Lambda 35, Perkin Elmer), using the absorbance at 410 nm. The concentration was obtained interpolating the absorbance value of the NP solution in a calibration curve made from Fe atomic spectroscopy standards. The [Fe] of the stock solution was approximately 10 mg/mL. The hydrodynamic diameter of the NPs in the aqueous solution was measured with a Nano-ZS Zetasizer (Malvern). The elemental composition of the dried NPs on Si substrates was measured by Rutherford backscattering spectroscopy (RBS), using a 2 MeV He beam and a detection angle of 165° and by RX energy dispersion spectroscopy.

The nuclear magnetic relaxation properties of the particles on water protons were obtained in a 3T clinical magnetic resonance scanner (SIGNA XDXT, G&E), imaging a phantom containing NP solutions with eight different concentrations, using spin eco or inversion recovery sequences.

2.4. Animal procedures

Intraperitoneal (i.p.) injection was adopted as the administration route for the *in vivo* protocols to ensure that exposure concentrations are in line with the target values. Intraperitoneal injections were conducted using a 3/10-mL U-100 BD Ultra-Fine™ Short Insulin Syringe 8 mm (5/16″) × 31G Short Needle (Becton Dickinson and Company, NJ, USA) according to the protocol established by Phelps et al. (2005). Briefly, the volume injected into the animal (mean injection volume of 10 μL) was adjusted to the fish bodyweight (mean mass of the animals was 0.5 ± 0.06 g/mean ± S.E.M.) to achieve 200 mg/kg. The animals of the control group received the same volume of saline solution and the animals of the buffer control group received the same volume of sodium citrate buffer. Anesthesia of the animals prior to the injection was obtained by immersion in a solution of tricaine (0.01%) until the animal showed a lack of motor coordination and reduced respiratory rate. The anesthetized fish was gently placed in a water-soaked gauze-wrapped hemostat with the abdomen facing up and the head of the fish positioned at the hinge of the hemostat (the pectoral fins were used as a landmark on the abdomen). The needle was inserted parallel to the spine in the midline of the abdomen posterior to the pectoral fins. The injection procedure was conducted in such a way as to guarantee that the animal did not spend more than 10 s out of the water. After the injection, the animals were placed in a separate tank with highly aerated dechlorinatedtap water (25 ± 2 °C) to facilitate recovery from the anesthesia. Saline solution was used as control. All the animals that recovered within 2–3 min following the injection continued in the experiment, while the animals

that did not recover during this period were discarded. One, 12, 24 and 48 h after the injection, the animals were euthanized by decapitation and the whole brains dissected for subsequent determination of AChE activity and molecular analysis. The concentrations of CLIO-NH_2 were chosen based on previous studies (Kim et al., 2005; Chertok et al., 2008 and Kumari et al., 2012).

2.5. Protein determination

The protein was determined by the Coomassie blue method according to Bradford (1976) using bovine serum albumin as standard.

2.6. Determination of AChE activity (EC 3.1.1.7)

Whole brains were removed by dissection (three whole brains for each sample) and homogenized on ice in 60 volumes (*v*/*w*) of Tris–citrate buffer (50 mM Tris, 2 mM EDTA, and 2 mM EGTA, pH 7.4, adjusted with citric acid), in a glass-Teflon homogenizer. The rate of acetylthiocholine hydrolysis (ACSCh, 0.88 mM) was assessed in a final volume of 300 μL with 11 mM phosphate buffer, pH 7.5, and 0.22 mM DTNB using a method previously described (Ellman et al., 1961). The samples containing protein (5 μg) and the reaction medium were pre-incubated for 10 min at 25 °C before the addition of substrate. The hydrolysis of substrate was monitored by the formation of thiolate dianion of DTNB at 412 nm for 2–3 min (intervals of 30 s) in a microplate reader. Controls without the homogenate preparation were performed in order to determine the non-enzymatic hydrolysis of the substrate. The linearity of absorbance against time and protein concentration was previously determined. The AChE activity was expressed as micromoles of thiocholine (SCh) released per hour per milligram of protein. All enzyme assays were evaluated in triplicate and at least three independent experiments were performed ($n \geq 3$).

2.7. Molecular analysis by RT-qPCR (quantitative PCR)

Gene expression analysis was carried out only when kinetic alteration occurred. For this reason, immediately after 24 h of intraperitoneal injection of the SPIONs, the animals were euthanized by decapitation. For each sample, a pool of at least three zebrafish whole brains was used. Total RNA was isolated using the TRIzol® reagent (Invitrogen) in accordance with the manufacturer's instructions. By calculating the ratio between absorbance values at 260 and 280 nm the purity of the RNA is asserted. The cDNA species were synthesized using ImPROm-II Reverse Transcriptase® (Promega, Madison, WI, USA), following the supplier's instructions. Quantitative PCR was performed using SYBR ® Green I (Invitrogen) to detect the synthesis of the double strand. The reactions had a total volume of 25 μL, using 12.5 μL of diluted cDNA (1:100 for *EF1α* and *Rlp13α*, and 1:20 for *ache*) containing a final concentration of 0.2× SYBR ® Green I (Invitrogen), 100 mM dNTP, 1× PCR buffer, 3 mM $MgCl_2$, 00:25 U Platinum ® Taq DNA Polymerase (Invitrogen) and 200 nM of each primer (Table 1). PCR reactions had the following conditions: 95 °C during 5 min for initial denaturation and polymerase activation, followed by 40 cycles of denaturation at 95 °C for 15 s, 60 °C to annealing for 35 s and extension for 15 s at 72 °C. At the end of cycles a melting curve analysis is added and the fluorescence was determined between 60 and 99 °C. The relative expression levels were determined with 7500 Fast Real-Time Software v.2.0.5 Sequence Detection System (Applied Biosystems). The efficiency for each sample was calculated using the software LinRegPCR 11.0 (Applied Biosystems) and the stability of *EF1α* and *Rlp13α* genes (M value) and the optimal number of reference genes according to the pairwise variation (V) were analyzed by geNorm (http://medgen.ugent.be/genorm/). The relative expression levels were determined using the method $2-\Delta\Delta CT$.

Table 1
Primers used in *RT-qPCR*.

Protein	Primer sequence (5′–3′)	Accession number
EF1α[a]	F-CTGGAGGCCAGCTCAAACAT R-ATCAAGAAGAGTAGTACCGCTAGCATTAC	NSDART00000023156
Rpl13α[a]	F-TCTGGAGGACTGTAAGAGGTATGC R-AGACGCACAATCTTGAGAGCAG	**NM_212784**
ache[b]	F-GCTAATGAGCAAAAGCATGTGGGCTTG R-TATCTGTGATGTTAAGCAGACGAGGCAGG	**NP_571921**
β-actin[b]	F-CGAGCTGTCTTCCCATCCA R-TCACCAACGTAGCTGTCTTTCTG	ENSDART00000055194

[a] According to Tang et al. (2007).
[b] According to Pereira et al. (2012).

2.8. Molecular analysis by RT^2 PCR Array

Total RNA from zebrafish whole brains ($n \geq 4$) was isolated with RNeasy® Mini Kit (Qiagen) and the DNase digestion step was made with the On-column DNase digestion step (Qiagen) in accordance with the manufacturer's instructions. The yield and quality of RNA samples were determined spectrophotometrically using 260 nm, 260/280 and 260/230 nm ratios and its integrity was confirmed by electrophoresis through an agarose gel 1.0%. One microgram of total RNA from the sample was reverse-transcribed into cDNA by RT2 First Strand (Qiagen) in a final volume of 20 μL. Custom RT^2 Profiler™ PCR (CAPZ 11803A) was used to analyze the expression profile of genes related to apoptosis, oxidative stress and inflammation, in accordance with the manufacturer's instructions. *EF1α* and *Rlp13α* were used as housekeeping genes and the total analyzed on a 7500 Fast Real-Time System Sequence Detection Software v.2.0.5 (Applied Biosystems). All genes represented by the array showed a single peak on the melting curve characteristic to the specific products.

2.9. Behavior analysis

The animals were intraperitoneally injected with CLIO-NH_2 or saline solution (control group) and after 24 h the behavior tests were performed as previously described (Gerlai et al., 2000; Egan et al., 2009). Zebrafish were placed individually in the experimental tanks (30 cm L × 15 cm H × 10 cm W). Once the animals were transferred to the experimental tank, they habituated for 30 s and the locomotor activity was recorded on video for 5 min. The tank was divided into equal sections (four vertical lines and one horizontal line) and during this time the following parameters were recorded: number of line crossings (vertical and horizontal lines), distance traveled (m), mean speed (m/s), absolute turn angle, time in upper zone, number of freezing (lack of movement for the period of 1 s or longer) and freezing duration. The videos were analyzed using ANYMaze software (Stoelting Co., Wood Dale, IL, USA).

2.10. Analysis of temporal absorption of iron by ICP-MS

The levels of iron in zebrafish brain were assessed by inductively-coupled plasma mass spectrometry (ICP-MS), according to the method described by Ashoka et al. (2009), with minor modifications. Briefly, pools of at least three brains were washed with saline solution (0.9%), and digested with 0.5 mL of 65% HNO_3 (Suprapur/Merck) and 0.1 mL of 37% HCl (ACS/Merck) in a glass tube. After, samples were placed for 2 h in a water bath at 85 °C and diluted to 5 mL with a 1% solution of HNO3. Subsequently, the samples were placed in the automatic sampler to be analyzed. The iron calibration curve was linear in the range of 10–1000 ppb (μg/L), and the results were expressed in microgram per sample ($n \geq 3$ brains).

2.11. Statistical analysis

Data was expressed as means ± S.E.M. and analyzed by one-way analysis of variance (ANOVA). Post-hoc comparisons were made using

Tukey's multiple comparison test, considering $p \leq 0.05$ as statistical significance.

3. Results

Typical size distribution of the synthesized CLIO-NH_2 nanoparticles is shown in Fig. 1. The magnetite core size, estimated from transmission electron microscopy images was 5.5 ± 1.4 nm (Fig. 1a). The number-averaged hydrodynamic diameter measured in an aqueous solution was 23 ± 8 nm (Fig. 1b). Elementary composition analysis of the particles indicated only the presence of Fe, O and trace elements from the sodium citrate buffer, (Na and Cl). The transversal to longitudinal relaxivity ratio R2/R1 was between 13 and 24 in the various batches produced.

Initially a dose–response curve was performed using CLIO-NH_2 concentrations from 20 to 200 mg/kg. Zebrafish brain AChE activity was evaluated 24 h after i.p. injections (Fig. 2). CLIO-NH_2 concentrations from 20 to 140 mg/kg did not alter AChE activity in zebrafish brains. However, the enzyme activity was significantly decreased at the highest tested concentration (200 mg/kg) when compared to the control (20.4%) and buffer control (18.2%) groups. Sequentially, a time-related curve was obtained using CLIO-NH_2 at 200 mg/kg. Zebrafish brain AChE activity was evaluated after one, 16, 24 and 48 h of exposure (Fig. 3). AChE activity was not affected at either one, 16 or 48 h after dosing. In contrast, AChE activity was reduced after 24 h after the exposure (27.47 ± 0.628 μmol Sch. h^{-1} mg $protein^{-1}$; $p = 0.0032$) when compared to the control (34.52 ± 0.952 μmol Sch. h^{-1} mg $protein^{-1}$) and buffer control (31.38 ± 1.39 μmol Sch. h^{-1} mg $protein^{-1}$) groups.

The decrease in brain AChE activity after 24 h exposure to 200 mg/kg of CLIO-NH_2 could be a consequence of transcriptional control and/or post-transcriptional modifications. In order to determine if *ache* transcriptional regulation had occurred, RT-qPCR analysis was performed. The results demonstrated that AChE transcript levels were not altered when compared to the control group (Fig. 4). This result indicates that the reduction of the AChE activity was not directly related to the inhibition of the gene *ache* expression.

As ACh is known to play an important role in the regulation of locomotor control, we further evaluated parameters of zebrafish swimming activity in the 5-min tank diving behavioral test. Exposure to 200 mg/kg of CLIO-NH_2 during 24 h decreased traveled distance (17.9 ± 2.36 m, $p = 0.0018$ compared to the control group 35.2 ± 3.96 m and to the buffer control group 22.4 ± 3.37 m), number of line crossings (240 ± 25.4, $p = 0.0141$ compared to the control group 418 ± 58.3 and to the buffer control group 242 ± 40.9) and mean speed (0.028 ± 0.00403 m/s, $p = 0.0041$ compared to the control group 0.0554 ± 0.00697 m/s and to the buffer control group 0.0356 ± 0.00560 m/s). Exposure to 200 mg/kg of CLIO-NH_2 during 24 h also decreased the absolute turn angle (47,500 ± 7240, $p = 0.0092$) when compared to the control group (78,200 ± 7110), whereas it did not differ statistically from the buffer control group (50,500 ± 7840) (Fig. 5). The time spent in the upper zone (54.87 ± 26.19 s) was not altered when compared to control (47.35 ± 10.87 s, $p = 0.7739$) and buffer control (69.05 ± 23.63 s) groups (data not shown). In addition, we did not find differences either in the number of freezing or freezing duration between the groups analyzed (data not show).

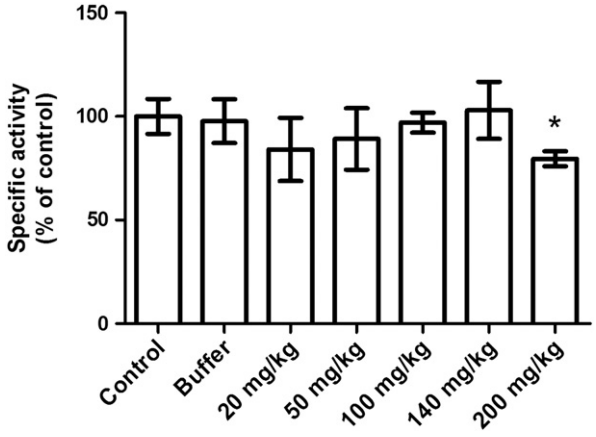

Fig. 2. *In vivo* effects of different concentrations of CLIO-NH_2 nanoparticles on ACh hydrolysis in zebrafish brain after 24 h exposure. Bars represent the mean ± S.E.M. The asterisk (*) indicates a significant difference compared to the control and buffer control groups. Data analyzed statically by one-way ANOVA, followed by Tukey's multiple comparison test. $p \leq 0.05$ denotes a significant difference from the control group.

The reduction in brain AChE activity and the impaired swimming performance parameters evaluated after 24 h exposure to 200 mg/kg of CLIO-NH_2 could be explained by iron accumulation in the brains. Inductively-coupled plasma mass spectrometry (ICP-MS) was employed to quantify iron levels in the brain tissue. The results indicated a significant higher level of ferric iron in zebrafish brains 24 h after treatment with CLIO-NH_2 (1.351 ± 0.1322 μg, $p = 0.0123$) when compared to the control (0.904 ± 0.0683 μg) and buffer control (0.761 ± 0.1067 μg) groups (Fig. 6).

In order to further investigate the mechanism involved in the brain toxicity caused by 24 h exposure to 200 mg/kg of CLIO-NH_2, the expression profile of a set of genes related to apoptosis, oxidative stress and inflammation was determined through RT^2 PCR Array analysis. The *casp8* (caspase 8), *casp9* (caspase 9) and *jun* (transcriptional factor AP-1) mRNAs were significantly increased when compared to control and

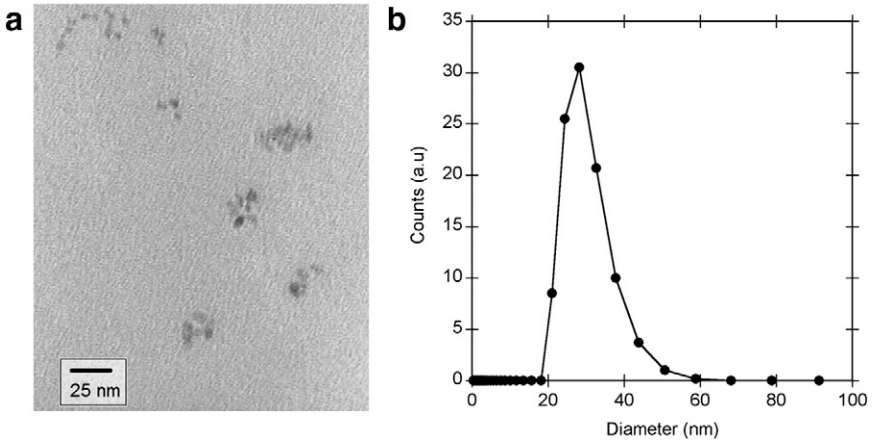

Fig. 1. a—Plan view TEM micrograph of the dried CLIO-NH_2 nanoparticles. b—Particle size distribution by number obtained by light scattering (Zetasizer) in a diluted aqueous solution at room temperature.

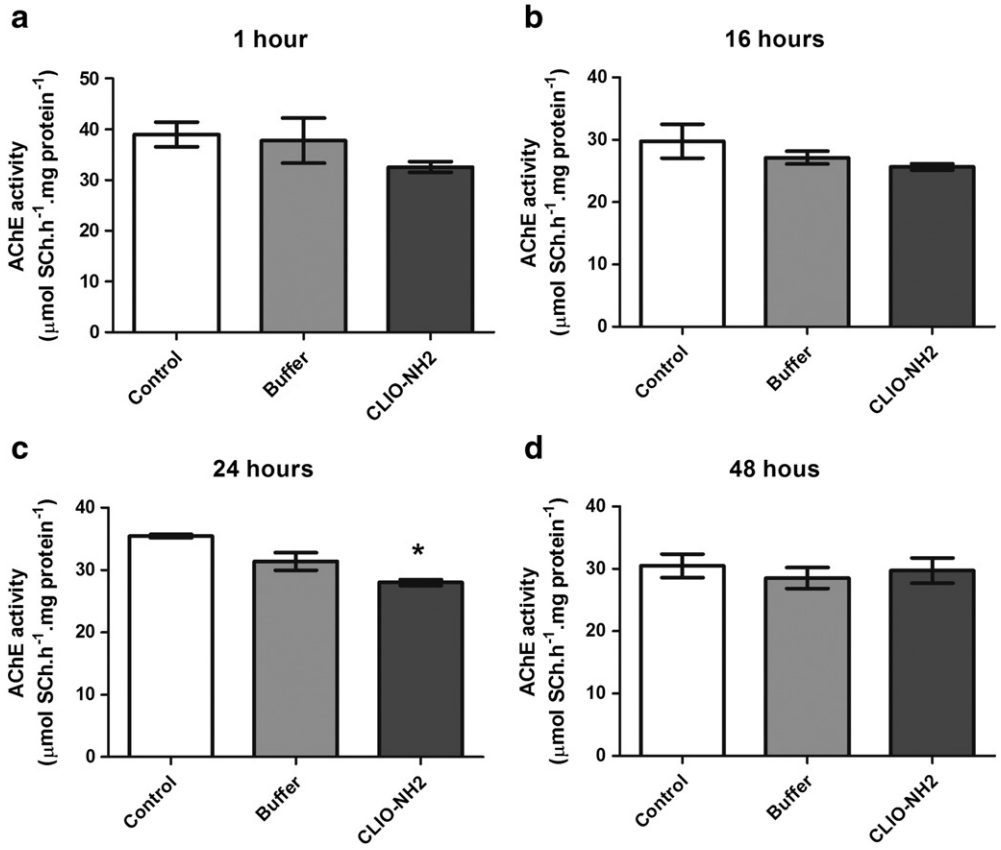

Fig. 3. *In vivo* effect of intraperitoneal injection of CLIO-NH_2 nanoparticles on zebrafish brain. a AChE activity 1 h after the exposure (36.7 ± 2.77 μmol Sch. h^{-1} mg $protein^{-1}$; control values). b AChE activity 16 h after the exposure (29.8 ± 2.72 μmol Sch. h^{-1} mg $protein^{-1}$; control values). c AChE activity 24 h after the exposure (34.52 ± 0.952 μmol Sch. h^{-1} mg $protein^{-1}$; control values). d AChE activity 48 h after the exposure (28.1 ± 1.26 μmol Sch. h^{-1} mg $protein^{-1}$; control values). *Bars* represent the mean ± SEM, performed in quadruplicate. The AChE activity was expressed as micromole of thiocholine released per hour per milligram of protein. Data were analyzed statically by one-way ANOVA, followed by Tukey's multiple comparison test. $p \leq 0.05$ denotes a significant difference from the control group.

buffer control groups. Of note, in one hand, the buffer exposure decreased the expression of all genes related to apoptosis analyzed, i.e. *bcl2* (B-cell leukemia/lymphoma 2), *casp3a* (apoptosis-related cysteine protease a), *casp8*, *casp9*, *tp53* (tumor protein p53) and *jun* when compared to the control group. One the other hand, 24 h exposure to 200 mg/kg of CLIO-NH_2 significantly increased the expression of the all genes analyzed when compared to the buffer control group (Fig. 7a). In addition, the buffer exposure also decreased the expression of all genes related to oxidative stress, i. e. *cat* (catalase), *gclc* (glutamate-cysteine ligase, catalytic subunit), *gpx1a* (glutathione peroxidase 1a), *gstp1* (glutathione S-transferase pi 1) and *sod2* (mitochondrial superoxide dismutase 2) when compared to the control group whereas the 24 h exposure to 200 mg/kg of CLIO-NH_2 significantly increased the expression of *gclc* and *gpx1a* when compared to the buffer control group (Fig. 7b). Finally, we did not find any differences in the expression of the genes associated with inflammation between the groups analyzed (data not shown).

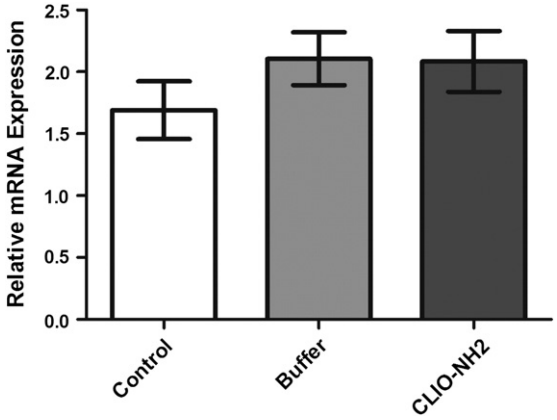

Fig. 4. RT-qPCR analysis. Relative *ache* mRNA expression on zebrafish brains 24 h after CLIO-NH_2 nanoparticle exposure (200 mg/kg). The asterisk (*) indicates a significant difference compared to the control group ($p \leq 0.05$).

4. Discussion

At present, one of the biggest concerns about the use of SPIONs remains around its toxicity. SPIONs synthetized of magnetite (Fe_3O_4) or maghemite (Fe_2O_3) have been extensively studied once these compounds have lower toxicity when compared to other transition metals such as cobalt, nickel or manganese (Tartaj et al., 2003). In addition, the surface coating can have important effects on SPION stability, aggregate size and cellular interaction which affects the SPION uptake in the intracellular medium (Raynal et al., 2004) resulting in toxic effects. The dextran-coated SPIONs were used in this study since they are recognized to improve biocompatibility, to enhance blood circulation and to reduce aggregation (Mahmoudi et al., 2012).

There are different methods of synthesis of NPs that allow greater control over the most varied characteristics and properties of the final product. Between them, the chemical routes such as co-precipitation, are simpler and more efficient to control the size, composition, and often the shape of the particle, being one of the most secure methods (Gupta and Wells, 2004; Gupta and Gupta, 2005). In this study, the

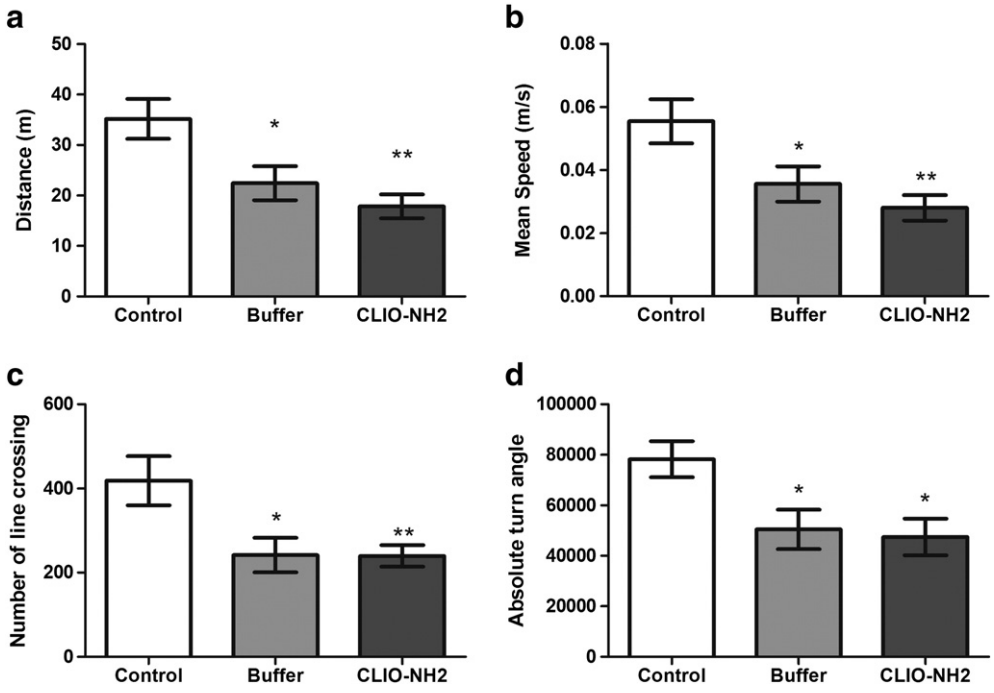

Fig. 5. Swimming performance. Effect of 24 h exposure to 200 mg/kg of CLIO-NH_2 nanoparticles on the distance traveled (a), mean speed (b), number of line crossings (c) and absolute turn angle (d) determined during 10 min of video recording in the tank-diving behavioral test. Bars represent the mean ± S.E.M. The asterisk (*) indicates a significant difference compared to the control group ($p \leq 0.05$) and (**) indicates a significant difference compared to the control and buffer control groups.

number-averaged hydrodynamic diameter of CLIO-NH_2 nanoparticles measured in an aqueous solution was 23 ± 8 nm which is in agreement with the size of SPIONs used in other studies (Naqvi et al., 2010; Kumari et al., 2013). The transversal to longitudinal relaxivity ratio R2/R1 was between 13 and 24, in the various batches of the dextran-coated SPIONs produced, which is close, but higher than those found for typical iron oxide contrast imaging formulations (Laurent et al., 2008; Geraldes and Laurent, 2009).

Some issues concerning the toxic effects caused by SPIONs exposure were already addressed using different species of fish as model organisms. For example, oxidative damage was demonstrated in the medaka (Japanese ricefish; *Oryzias latipes*) embryos exposed to nano-iron NPs in a dose-dependent manner (Li et al., 2009), and to nanoscale iron oxide (nFe_3O_4) at environmentally relevant concentrations (from 0.5 to 5 mg/L) (Chen et al., 2012). Zhu et al. (2012) showed that ≥10 mg/L of SPIONs exposure instigated developmental toxicity in zebrafish embryos. In the present study, we have evaluated the effect of different CLIO-NH_2 doses (20, 50, 100, 140 and 200 mg/kg) and different times of exposure (one, 16, 24 and 48 h) on AChE activity and *ache* expression in zebrafish brain. In the concentrations tested, only the animals exposed to 200 mg/kg for 24 h have shown decreased AChE activity. The RT-qPCR results suggested that inhibition of brain AChE is not directly related with the transcriptional control and it was probably due to a post-transcriptional or even a post-translational event.

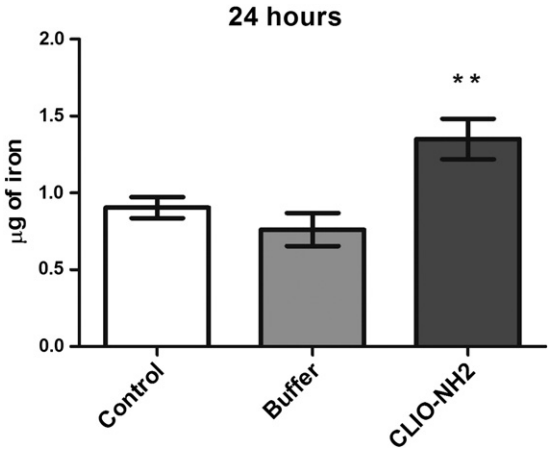

Fig. 6. Effect of CLIO-NH_2 nanoparticle exposure in zebrafish brain. The levels of iron in zebrafish brain are indicated in microgram. Bars represent the mean ± S.E.M. The double asterisks (**) indicate a significant difference compared to the control and buffer control groups. Data were analyzed statistically by one-way ANOVA, followed by Tukey's multiple comparison test. $p \leq 0.05$ denotes a significant difference from the control group.

To the best of our knowledge, only two other studies have evaluated the toxic effects of SPION exposure over brain AChE activity. Repeated oral dose of Fe_2O_3-30 nanoparticles during 28 days caused a significant inhibition of brain AChE activity in a female Wistar rat model (Kumari et al., 2012). Acute oral exposure to Fe_2O_3 nanoparticles also resulted in a significant inhibition of brain AChE activity, as well as in red blood cells in a female Wistar rat model (Kumari et al., 2013). The results reported herein are in accordance with these two studies and suggest that synaptic transmission can be affected by exposure to SPIONs.

It is well-documented that inhibition of AChE mostly leads to an increase in the ACh accumulation in the brain leading to an overstimulation of cholinergic receptors. As a result, a decline in neural and muscular control occurs. There are some reports in the literature linking inhibition of the zebrafish AChE activity and behavioral changes with the exposure to pollutants and/or toxic agents. For instance, exposure to 2.4 µg endosulfan/L (organochlorine pesticide) for 96 h, a condition that resulted in brain AChE inhibition, also impaired exploratory parameters of adult zebrafish (Pereira et al., 2012). The organophosphorus pesticide chlorpyrifos (300 nM dissolved in water) over the first five days of embryonic and larval development of zebrafish reduced both AChE (81%) and locomotor activities (35%) (Yen et al., 2011). In the present study, exposure to 200 mg/kg of CLIO-NH_2 during 24 h, a condition that inhibited the brain AChE activity, also impaired all the evaluated parameters of zebrafish swimming activity, i.e. decreased traveled distance, mean speed, number of line crossings, and turn angle. It is

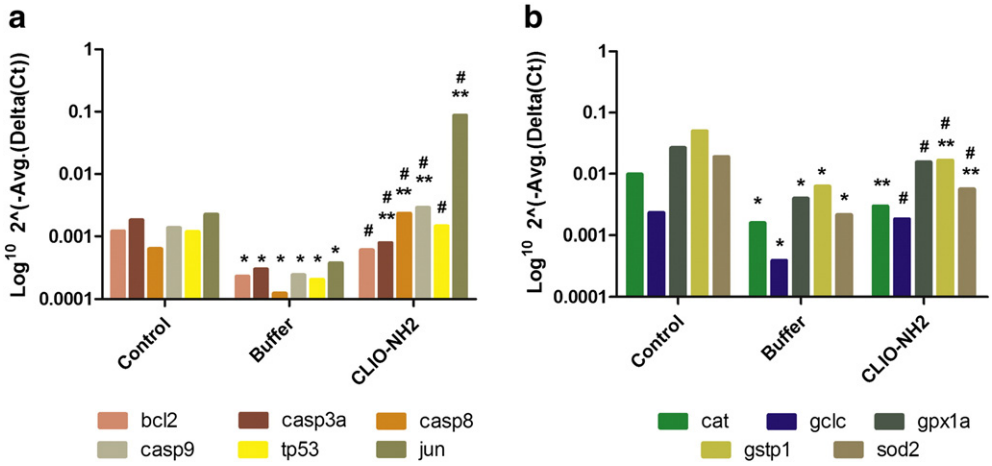

Fig. 7. RT^2 PCR Array analysis. Relative mRNA levels of apoptosis (a) and oxidative stress (b) related genes on zebrafish brain 24 h after CLIO-NH_2 nanoparticle exposure (200 mg/kg). Results are shown in Log10 2^(−Avg.(Delta(Ct)). The asterisk (*) indicates a significant difference compared to the control group, double asterisk (**) indicates a significant difference compared to the control and buffer control groups and hashtag (#) indicates a significant difference compared to the buffer control group.

important to highlight that the exposure to the buffer control group (sodium citrate buffer) was also harmful to the fishes suggesting that part of the toxic effects found in the behavior tests are due to the buffer used to store the CLIO-NH_2 nanoparticles. Sodium citrate on the surface of gold nanoparticles induced cytotoxicity in alveolar type-II cell lines (Uboldi et al., 2009) and decreased cell viability and proliferation of the two human endothelial cells lines (from the vasculature and blood brain barrier) (Freese et al., 2012). Nevertheless, the nanoparticle exposure decreased traveled distance, mean speed, and number of line crossings in a way that was statistically different from the buffer control group suggesting combined effects. These findings showed that CLIO-NH_2 exposure impaired zebrafish's exploratory performance and possibly weakened their ecological and interspecific interaction.

Once internalized, the intracellular mechanisms involved in the degradation of SPIONs are lysosome-mediated (Arbab et al., 2005; Lévy et al., 2010, releasing free Fe (III) into the cellular medium via divalent cationic transport. The iron is then stored in the body with the help of the iron-regulating proteins. The transport of iron in the blood is performed by plasma protein transferrin and can accumulate in the case of iron overload (Wahajuddin and Arora, 2012). In order to investigate the hypothesis raised, ICP-MS analysis was carried out. The results showed a significant higher level of ferric iron in zebrafish brains after 24 h of treatment with CLIO-NH_2. This scenario was reversed in the next 24 h (AChE activity was not down-regulated after 48 h exposure to 200 mg/kg of CLIO-NH_2) where iron accumulated in brain might be metabolized or excreted by the body allowing cells to return to homeostasis.

Taking into account that the excessive accumulation of free iron can causes toxicity via generation of reactive oxygen species (ROS) and induction of the cell death (for review see Dixon and Stockwell, 2014) we further investigated the mechanism involved in the brain toxicity caused by 24 h exposure to 200 mg/kg of CLIO-NH_2 by evaluating the expression profile of a set of genes related to apoptosis, oxidative stress and inflammation. RT^2 PCR Array analysis has shown that the *casp8*, *casp9* and *jun* transcripts were significantly increased after 24 h exposure to 200 mg/kg of CLIO-NH_2 when compared to control and buffer control groups. Furthermore, the buffer exposure decreased the expression of all genes related to apoptosis and to oxidative stress analyzed when compared to the control group. In contrast, 24 h exposure to 200 mg/kg of CLIO-NH2 significantly increased the expression of the all genes related to apoptosis and *gclc* and *gpx1a* genes when compared to the buffer control group. Here again, it is important to notice that sodium citrate buffer induced important effects *per se*. Nevertheless, these findings suggest that apoptotic events had occurred following 24 h exposure to 200 mg/kg of CLIO-NH2. Our results are in agreement with other studies where iron overload induced apoptosis, for example, in macrophages (Pirdel et al., 2007; Naqvi et al., 2010) and in hepatocyte cells (Allameh and Amini-harandi, 2008). Moreover, caspase activation after iron treatment has been previously reported in the cell culture of endothelial aortic bovine cells (Carlini et al., 2006) and in an *in vivo* study using Mongolian gerbil (*Meriones unguiculatus*) as a model organism (Wang et al., 2011).

Studies often classified SPIONs as biocompatible without severe neurotoxic effects (Jain et al., 2008; Chertok et al., 2008; Yu et al., 2008 and Schlachter et al., 2011). In addition, it has been mostly shown that toxic effects were associated with acute iron overload (Patruta and Horl, 1999) caused only by high dose SPION exposure (Kumari et al., 2012; Kumari et al., 2013). The results present herein reinforce these findings.

In summary, the results presented in this article provide further experimental evidence that SPION exposure can be transiently neurotoxic. Adult zebrafish exposed 24 h to 200 mg/kg showed down-regulation in brain AChE activity, impaired swimming performance parameters, significant higher level of ferric iron in the brains and induction of *casp8*, *casp 9* and *jun* genes. Altogether our findings suggest brain toxicity by the inhibition of acetylcholinesterase and induction of apoptosis and certainly could help to establish the upper save limits to be used in nanomedicine.

Conflict of interest

The authors declare they have no conflict of interest.

Acknowledgments

This work was supported by Conselho Nacional de Desenvolvimento Científico e Tecnológico (CNPq) (grant number 552131/2011-3), DECIT/SCTIEMS through CNPq and Fundação de Amparo à Pesquisa do Estado do Rio Grande do Sul (FAPERGS) (grant number 10/0036-5—PRONEX), FAPERGS (grant number 11/2037-9 PRONEM) and by the FINEP research grant "Implantação, Modernização e Qualificação de Estrutura de Pesquisa da PUCRS" (PUCRSINFRA) (grant number) 01.11.0014-00. GMTO, TCBP, JWB and FLP were recipients of fellowships from Coordenação de Aperfeiçoamento de Pessoal de Nível Superior (CAPES). LWK was recipient of fellowship from the CAPES/PNPD Program. EMN was recipient of fellowship from Hewlett-Packard (TECNOPUC/PUCRS). CDB, NRSB, RMP and MRB are Research Career Awardees of the CNPq.

References

Allameh, A., Amini-harandi, A., 2008. Iron overload induced apoptotic cell death in isolated rat hepatocytes mediated by reactive oxygen species. Iran. J. Pharm. Res. 7, 115–121.

Arbab, A.S., Wilson, L.B., Ashari, P., Jordan, E.K., Lewis, B.K., Frank, J.A., 2005. A model of lysosomal metabolism of dextran coated superparamagnetic iron oxide (SPIO) nanoparticles: implications for cellular magnetic resonance imaging. NMR Biomed. 18, 383–389.

Ashoka, S., Peake, B.M., Bremner, G., Hageman, K.J., Reid, M.R., 2009. Comparison of digestion methods for ICP-MS determination of trace elements in fish tissues. Anal. Chim. Acta. 653, 191–199.

Bertrand, C., Chatonnet, A., Takke, C., Yan, Y.L., Postlethwait, J., Toutant, J.P., Cousin, X., 2001. Zebrafish acetylcholinesterase is encoded by a single gene localized on linkage group 7. Gene structure and polymorphism; molecular forms and expression pattern during development. J. Biol. Chem. 276, 464–474.

Bradford, M.M., 1976. A rapid and sensitive method for the quantitation of microgram quantities of protein utilizing the principle of protein-dye binding. Anal. Biochem. 72, 248–254.

Carlini, R.G., Alonzo, E., Bellorin-Font, E., Weisinger, J.R., 2006. Apoptotic stress pathway activation mediated by iron on endothelial cells in vitro. Nephrol. Dial. Transplant. 21, 3055–3061.

Chen, P.-J., Tan, S.-W., Wu, W.-L., 2012. Stabilization or oxidation of nanoscale zerovalent iron at environmentally relevant exposure changes bioavailability and toxicity in medaka fish. Environ. Sci. Technol. 46, 8431–8439.

Chertok, B., Moffat, B.A., David, A.E., Yu, F., Bergemann, C., Ross, B.D., Yang, V.C., 2008. Iron oxide nanoparticles as a drug delivery vehicle for MRI monitored magnetic targeting of brain tumors. Biomaterials 29, 487–496.

Chouly, C., Pouliquen, D., Lucet, I., Jeune, J.J., Jallet, P., 1996. Development of superparamagnetic nanoparticles for MRI: effect of particle size, charge and surface nature on biodistribution. J. Microencapsul. 13, 245–255.

Dixon, S.J., Stockwell, B.R., 2014. The role of iron and reactive oxygen species in cell death. Nat. Chem. Biol. 10, 9–17.

Egan, R.J., Bergner, C.L., Hart, P.C., Cachat, J.M., Canavello, P.R., Elegante, M.F., Elkhayat, S.I., Bartels, B.K., Tien, A.K., Tien, D.H., Mohnot, S., Beeson, E., Glasgow, E., Amri, H., Zukowska, Z., Kalueff, A.V., 2009. Understanding behavioral and physiological phenotypes of stress and anxiety in zebrafish. Behav. Brain Res. 205, 38–44.

Ellman, G.L., Courtney, K.D., Andres, V., Feather-Stone, R.M., 1961. A new and rapid colorimetric determination of acetylcholinesterase activity. Biochem. Pharmacol. 7, 88–95.

Freese, C., Uboldi, C., Gibson, M.I., Unger, R.E., Weksler, B.B., Romero, I.A., Couraud, P.-O., Kirkpatrick, C.J., 2012. Uptake and cytotoxicity of citrate-coated gold nanospheres: comparative studies on human endothelial and epithelial cells. Part Fibre Toxicol. 9, 23.

Geraldes, C.F.G.C., Laurent, S., 2009. Classification and basic properties of contrast agents for magnetic resonance imaging. Contrast Media Mol. Imaging 4, 1–23.

Gerlai, R., Lahav, M., Guo, S., Rosenthal, A., 2000. Drinks like a fish: zebra fish (*Danio rerio*) as a behavior genetic model to study alcohol effects. Pharmacol. Biochem. Behav. 67, 773–782.

Gupta, A.K., Gupta, M., 2005. Synthesis and surface engineering of iron oxide nanoparticles for biomedical applications. Biomaterials 26, 3995–4021.

Gupta, A.K., Wells, S., 2004. Surface-modified superparamagnetic nanoparticles for drug delivery: preparation, characterization, and cytotoxicity studies. IEEE Trans. Nanobiosci. 3, 66–73.

Hanini, A., Schmitt, A., Kacem, K., Chau, F., Ammar, S., Gavard, J., 2011. Evaluation of iron oxide nanoparticle biocompatibility. Int. J. Nanomedicine 6, 787–794.

Ito, A., Shinkai, M., Honda, H., Kobayashi, T., 2005. Medical application of functionalized magnetic nanoparticles. J. Biosci. Bioeng. 100, 1–11.

Jain, T.K., Reddy, M.K., Morales, M.A., Leslie-Pelecky, D.L., Labhasetwar, V., 2008. Biodistribution, clearance, and biocompatibility of iron oxide magnetic nanoparticles in rats. Mol. Pharm. 5, 316–327.

Kim, S.-S., Kim, S.-T., Yoon, Y.-C., Lee, K.-S., 2005. Magnetic, dielectric, and microwave absorbing properties of iron particles dispersed in rubber matrix in gigahertz frequencies. J. Appl. Phys. 97, 10 (F905).

Kist, L.W., Rosemberg, D.B., Pereira, T.C.B., de Azevedo, M.B., Richetti, S.K., de Castro Leão, J., Yunes, J.S., Bonan, C.D., Bogo, M.R., 2012. Microcystin-LR acute exposure increases AChE activity via transcriptional ache activation in zebrafish (*Danio rerio*) brain. Comp. Biochem. Physiol. C. Toxicol. Pharmacol. 155, 247–252.

Kumari, M., Rajak, S., Singh, S.P., Kumari, S.I., Kumar, P.U., Murty, U.S.N., Mahboob, M., Grover, P., Rahman, M.F., 2012. Repeated oral dose toxicity of iron oxide nanoparticles: biochemical and histopathological alterations in different tissues of rats. J. Nanosci. Nanotechnol. 12, 2149–2159.

Kumari, M., Rajak, S., Singh, S.P., Murty, U.S.N., Mahboob, M., Grover, P., Rahman, M.F., 2013. Biochemical alterations induced by acute oral doses of iron oxide nanoparticles in Wistar rats. Drug Chem. Toxicol. 36, 296–305.

Laurent, S., Forge, D., Port, M., Roch, A., Robic, C., Vander Elst, L., Muller, R.N., 2008. Magnetic iron oxide nanoparticles: synthesis, stabilization, vectorization, physicochemical characterizations, and biological applications. Chem. Rev. 108, 2064–2110.

Lévy, M., Lagarde, F., Maraloiu, V.-A., Blanchin, M.-G., Gendron, F., Wilhelm, C., Gazeau, F., 2010. Degradability of superparamagnetic nanoparticles in a model of intracellular environment: follow-up of magnetic, structural and chemical properties. Nanotechnology 21, 395103.

Li, H., Zhou, Q., Wu, Y., Fu, J., Wang, T., Jiang, G., 2009. Effects of waterborne nano-iron on medaka (*Oryzias latipes*): antioxidant enzymatic activity, lipid peroxidation and histopathology. Ecotoxicol. Environ. Saf. 72, 684–692.

Lu, A.-H., Salabas, E.L., Schüth, F., 2007. Magnetic nanoparticles: synthesis, protection, functionalization, and application. Angew. Chem. Int. Ed. Engl. 46, 1222–1244.

Mahmoudi, M., Hofmann, H., Rothen-Rutishauser, B., Petri-Fink, A., 2012. Assessing the in vitro and in vivo toxicity of superparamagnetic iron oxide nanoparticles. Chem. Rev. 112, 2323–2338.

Naqvi, S., Samim, M., Abdin, M., Ahmed, F.J., Maitra, A., Prashant, C., Dinda, A.K., 2010. Concentration-dependent toxicity of iron oxide nanoparticles mediated by increased oxidative stress. Int. J. Nanomedicine 5, 983–989.

Oliveira, R., da, L., Seibt, K.J., Rico, E.P., Bogo, M.R., Bonan, C.D., 2011. Inhibitory effect of lithium on nucleotide hydrolysis and acetylcholinesterase activity in zebrafish (*Danio rerio*) brain. Neurotoxicol. Teratol. 33, 651–657.

Patruta, S.I., Horl, W.H., 1999. Iron and infection. Kidney Int. 55, S125–S130.

Pereira, V.M., Bortolotto, J.W., Kist, L.W., Azevedo, M.B. De, Fritsch, R.S., Oliveira, R.D.L., Pereira, T.C.B., Bonan, C.D., Vianna, M.R., Bogo, M.R., 2012. Endosulfan exposure inhibits brain AChE activity and impairs swimming performance in adult zebrafish (Danio rerio). Neurotoxicology 33, 469–475.

Phelps, H.A., Runft, D.L., Neely, M.N., 2005. Adult Zebrafish Model of Streptococcal Infection, in: Current Protocols in Microbiology. John Wiley & Sons, Inc.

Pirdel, L., Hosseini, A., Tiraihi, T., 2007. Role of iron overload in apoptosis of Balb/c mice macrophages infected with leishmania major in vitro. Yakhteh Med. J. 9, 196–201.

Raynal, I., Prigent, P., Peyramaure, S., Najid, A., Rebuzzi, C., Corot, C., 2004. Macrophage endocytosis of superparamagnetic iron oxide nanoparticles: mechanisms and comparison of ferumoxides and ferumoxtran-10. Invest. Radiol. 39.

Richetti, S.K., Rosemberg, D.B., Ventura-Lima, J., Monserrat, J.M., Bogo, M.R., Bonan, C.D., 2011. Acetylcholinesterase activity and antioxidant capacity of zebrafish brain is altered by heavy metal exposure. Neurotoxicology 32, 116–122.

Rico, E.P., Rosemberg, D.B., Senger, M.R., Arizi, M.D.B., Bernardi, G.F., Dias, R.D., Bogo, M.R., Bonan, C.D., 2006. Methanol alters ecto-nucleotidases and acetylcholinesterase in zebrafish brain. Neurotoxicol. Teratol. 28, 489–496.

Rico, E.P., Rosemberg, D.B., Dias, R.D., Bogo, M.R., Bonan, C.D., 2007. Ethanol alters acetylcholinesterase activity and gene expression in zebrafish brain. Toxicol. Lett. 174, 25–30.

Schlachter, E.K., Widmer, H.R., Bregy, A., Lönnfors-Weitzel, T., Vajtai, I., Corazza, N., Bernau, V.J.P., Weitzel, T., Mordasini, P., Slotboom, J., Herrmann, G., Bogni, S., Hofmann, H., Frenz, M., Reinert, M., 2011. Metabolic pathway and distribution of superparamagnetic iron oxide nanoparticles: in vivo study. Int. J. Nanomedicine 6, 1793–1800.

Senger, M.R., Seibt, K.J., Ghisleni, G.C., Dias, R.D., Bogo, M.R., Bonan, C.D., 2011. Aluminum exposure alters behavioral parameters and increases acetylcholinesterase activity in zebrafish (*Danio rerio*) brain. Cell Biol. Toxicol. 27, 199–205.

Singh, N., Jenkins, G.J.S., Asadi, R., Doak, S.H., 2010. Potential toxicity of superparamagnetic iron oxide nanoparticles (SPION). Nanomedicine Rev. 1, 1–15.

Soreq, H., Seidman, S., 2001. Acetylcholinesterase–new roles for an old actor. Nat. Rev. Neurosci. 2, 294–302.

Tang, R., Dodd, A., Lai, D., McNabb, W.C., Love, D.R., 2007. Validation of zebrafish (*Danio rerio*) reference genes for quantitative real-time RT-PCR normalization. Acta Biochim. Biophys. Sin. 39, 384–390.

Tartaj, P., Morales, M.A.D.P., Veintemillas-Verdaguer, S., Gonz lez-Carre O, T., Serna, C.J., 2003. The preparation of magnetic nanoparticles for applications in biomedicine. J. Phys. D. Appl. Phys. 36, R182–R197.

Uboldi, C., Bonacchi, D., Lorenzi, G., Hermanns, M.I., Pohl, C., Baldi, G., Unger, R.E., Kirkpatrick, C.J., 2009. Gold nanoparticles induce cytotoxicity in the alveolar type-II cell lines A549 and NCIH441. Part Fibre Toxicol. 6, 18.

Van Dyk, J.S., Pletschke, B., 2011. Review on the use of enzymes for the detection of organochlorine, organophosphate and carbamate pesticides in the environment. Chemosphere 82, 291–307.

Wahajuddin, Arora, S., 2012. Superparamagnetic iron oxide nanoparticles: magnetic nanoplatforms as drug carriers. Int. J. Nanomedicine 7, 3445–3471.

Wang, Y.X., Hussain, S.M., Krestin, G.P., 2001. Superparamagnetic iron oxide contrast agents: physicochemical characteristics and applications in MR imaging. Eur. Radiol. 11, 2319–2331.

Wang, Y., Wu, M., Al-Rousan, R., Liu, H., Fannin, J., Paturi, S., Arvapalli, R.K., Katta, A., Kakarla, S.K., Rice, K.M., Triest, W.E., Blough, E.R., 2011. Iron-induced cardiac damage: role of apoptosis and deferasirox intervention. J. Pharmacol. Exp. Ther. 336, 56–63.

Wunderbaldinger, P., Josephson, L., Weissleder, R., 2002. Crosslinked iron oxides (CLIO): a new platform for the development of targeted MR contrast agents. Acad. Radiol. 9 (Suppl. 2), S304–S306.

Yen, J., Donerly, S., Levin, E.D., Linney, E.A., 2011. Differential acetylcholinesterase inhibition of chlorpyrifos, diazinon and parathion in larval zebrafish. Neurotoxicol. Teratol. 33, 735–741.

Yu, M.K., Jeong, Y.Y., Park, J., Park, S., Kim, J.W., Min, J.J., Kim, K., Jon, S., 2008. Drug-loaded superparamagnetic iron oxide nanoparticles for combined cancer imaging and therapy in vivo. Angew. Chem. Int. Ed. Engl. 47, 5362–5365.

Zhu, X., Tian, S., Cai, Z., 2012. Toxicity assessment of iron oxide nanoparticles in zebrafish (*Danio rerio*) early life stages. PLoS ONE 7, e46286.